Online Appendix to Routing in Line Networks with Handling Times

Gabriel Deza, Michal Tzur, Tal Raviv

School of Industrial and Intelligent Systems Engineering, Tel Aviv University

gabrieldeza@mail.tau.ac.il, tzurm@tauex.tau.ac.il, talraviv@tauex.tau.ac.il

Appendix

This online appendix is organized into three parts. Appendix A contains the proofs. Appendix B discusses infeasibility and presents the complete SDP formulation used to compute the residual-frontier lower bound. Appendix C provides additional figures and details on the synthetic and real-world instances.

Appendix A: Proofs

Proof of Proposition 1. Let $(\mathbf{x}^*, \Delta^*)$ be an optimal solution to $(\mathbf{RD}_{x,\Delta})$. Keeping $\mathbf{x}^*$ fixed, choose Δ^* to minimize total dwell time among dwell-time vectors preserving feasibility and optimality. Suppose that for some line $l \in \mathcal{L}$ and node $i \in \mathcal{N}(l)$, constraint (1e) has slack, that is,

$$\sum_{k \in \mathcal{D}} \left(\alpha t_i^{*kl} + \beta u_i^{*kl}\right) < \Delta_i^{*l}\, a_l \frac{T}{C_l + \sum_{j \in \mathcal{N}(l)} \Delta_j^{*l}}.$$

In particular, the right-hand side is positive, so $\Delta_i^{*l} > 0$. Consider a perturbation that decreases Δ_i^{*l} slightly by setting

$$\hat{\Delta}_i^l = \Delta_i^{*l} - \epsilon, \qquad \epsilon \in (0, \Delta_i^{*l}),$$

and keep all other variables unchanged, i.e., $(\hat{\mathbf{x}}, \hat{\Delta}) = (\mathbf{x}^*, \Delta^*)$ except at (i, l).

This perturbation does not affect flow conservation. Moreover, any constraints whose right-hand side depends on the line cycle time through $C_l + \sum_{j \in \mathcal{N}(l)} \Delta_j^l$ become no tighter, since this denominator decreases when Δ_i^l is reduced. For constraint (1e) at (i, l), the left-hand side is unchanged, while the right-hand side varies continuously in Δ_i^l. Since the constraint is slack at $(\mathbf{x}^*, \Delta^*)$, it remains satisfied for all sufficiently small $\epsilon > 0$. Hence, $(\hat{\mathbf{x}}, \hat{\Delta})$ is feasible.

Finally, the objective is nondecreasing in each dwell time, so this perturbation cannot increase its value. The perturbed solution therefore remains optimal but has strictly smaller total dwell time, contradicting our choice of Δ^*. Thus, all handling constraints are tight in the chosen optimal solution. □

Proof of Proposition 2. For necessity, suppose $\mathbf{\Delta}$ is feasible. Write $H_l = \sum_{i \in \mathcal{N}(l)} h_i^l$ and $f_l = T a_l / (C_l + \sum_{i \in \mathcal{N}(l)} \Delta_i^l)$. Summing the handling constraints gives

$$H_l \le f_l \sum_i \Delta_i^l = T a_l - C_l f_l < T a_l.$$

Hence $f_l \le (T a_l - H_l)/C_l$, and the vehicle-capacity constraints imply (3). Conversely, suppose (2)–(3) hold. Consider constraint (1e) at equality and sum it over a line $l \in \mathcal{L}$:

$$\sum_{i \in \mathcal{N}(l)} \sum_{k \in \mathcal{D}} \left(\alpha t_i^{kl} + \beta u_i^{kl}\right) = \sum_{i \in \mathcal{N}(l)} \Delta_i^l a_l \frac{T}{C_l + \sum_{j \in \mathcal{N}(l)} \Delta_j^l} \tag{EC.1}$$

Factoring out $\sum_{q\in\mathcal{N}(l)}\Delta_q^l$ gives the total dwell time along the line:

$$\sum_{q\in\mathcal{N}(l)}\Delta_q^l=\frac{C_lH_l}{Ta_l-H_l}.$$

This expression is valid only when the denominator is strictly positive, which gives condition (2). Substituting the total dwell time back into the equality for hub $i\in\mathcal{N}(l)$ gives

$$h_i^l=\Delta_i^l\frac{Ta_l}{C_l+\frac{C_lH_l}{Ta_l-H_l}}=\Delta_i^l\frac{Ta_l-H_l}{C_l}.$$

Rearranging yields (4). Substituting the same expression for the line frequency into the vehicle-capacity constraints gives (3). For any feasible dwell-time vector, $\Delta_i^l\geq h_i^l/f_l\geq C_lh_i^l/(Ta_l-H_l)=\Delta_i^{*l}$. Since the objective is nondecreasing in each dwell time, the displayed vector minimizes total travel time for the fixed flow. □

Proof of Proposition 3. Let $x^\star=(d^\star,t^\star,u^\star)$ be optimal. We first show that one never boards and alights simultaneously for the same (i,k,l). Suppose $t_i^{kl\star}>0$ and $u_i^{kl\star}>0$ for some (i,k,l), and set $\varepsilon=\min\{t_i^{kl\star},u_i^{kl\star}\}>0$. Define $\tilde{x}$ by decreasing both variables at (i,k,l), i.e., $\tilde{t}_i^{kl}=t_i^{kl\star}-\varepsilon$, $\tilde{u}_i^{kl}=u_i^{kl\star}-\varepsilon$, and leaving all other variables unchanged.

This preserves feasibility. The node-balance and line-flow equalities depend on $t_i^{kl}-u_i^{kl}$, which is unchanged. The dwell-time inequality depends on $\sum_{i,k}(\alpha t_i^{kl}+\beta u_i^{kl})$ and therefore becomes looser. The capacity inequality depends on the same sum of t-variables and its right-hand side weakly increases when t_i^{kl} is reduced. Nonnegativity holds by the choice of ε.

Moreover, the objective is strictly increasing in each t_i^{kl} and u_i^{kl} on the feasible set, since these variables enter the handled-volume terms $H_l=\sum_{i,k}(\alpha t_i^{kl}+\beta u_i^{kl})$ with positive coefficients, and the corresponding cost terms are increasing in H_l (the linear travel cost is independent of t and u). Hence $F(\tilde{x})<F(x^\star)$, contradicting optimality. Therefore, for all (i,k,l), $t_i^{kl\star}>0$ implies $u_i^{kl\star}=0$, and $u_i^{kl\star}>0$ implies $t_i^{kl\star}=0$.

Fix any (i,k,l). Flow conservation (5c) gives $d_{i_i}^{kl\star}+t_i^{kl\star}=d_{ii_+}^{kl\star}+u_i^{kl\star}$. If $u_i^{kl\star}>0$, then $t_i^{kl\star}=0$ and thus $d_{i_i}^{kl\star}=d_{ii_+}^{kl\star}+u_i^{kl\star}\geq u_i^{kl\star}$. If $u_i^{kl\star}=0$, the inequality $d_{i_i}^{kl\star}\geq u_i^{kl\star}$ is trivial by nonnegativity. Hence $d_{i_i}^{kl\star}\geq u_i^{kl\star}$ for all (i,k,l), and summing over k yields $X_i^{l\star}\geq U_i^{l\star}$ for all $i\in\mathcal{N}(l)$ and $l\in\mathcal{L}$. □

Proof of Theorem 1. For any $x\in\mathcal{X}$, define $\gamma(x):=g(x)-g_c\geq 0$. Then x is feasible for the definition of $m(\gamma(x))$, and therefore

$$r(x)\geq m(\gamma(x)).$$

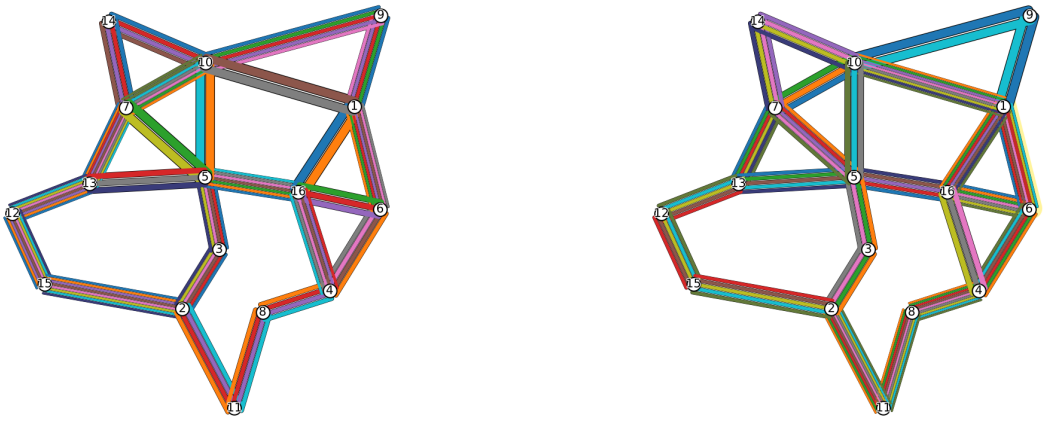
Thus

$$F^*\geq g_c+\min_{\gamma\geq 0}\{\gamma+m(\gamma)\}.$$

Conversely, for any $\gamma\geq 0$ and any $\eta>0$, choose an η-optimal solution x_γ^η for $m(\gamma)$, so that $r(x_\gamma^\eta)\leq m(\gamma)+\eta$ and $g(x_\gamma^\eta)\leq g_c+\gamma$. Then

$$F(x_\gamma^\eta)=g(x_\gamma^\eta)+r(x_\gamma^\eta)\leq g_c+\gamma+m(\gamma)+\eta.$$

Letting $\eta\downarrow 0$ and minimizing over γ gives the reverse inequality. Since x_c is feasible, $F^*\leq F(x_c)=g_c+r_c$. If $\gamma>r_c$, then $\gamma+m(\gamma)\geq\gamma>r_c$, so such values of γ cannot improve on the incumbent. Hence the minimization can be restricted to $[0,r_c]$. Subtracting from $F_c=g_c+r_c$ gives the second result. □



(a) Feasible baseline (b) Infeasible baseline due to arc capacity overload.

Figure EC.1 **Two different line concepts admitting feasible and infeasible baseline routing solutions once handling is accounted for.**

Appendix B: Infeasibility and Frontier bound details

Baseline infeasibility The handling-ignorant baseline can become infeasible once handling times are imposed because handling affects the effective capacity of each line. Figure EC.1a shows a P_{16} line network for which the baseline routing remains feasible after handling times are accounted for. In this case, the handling workload induced by the baseline routing remains sufficiently dispersed, so all temporal and effective-capacity constraints are satisfied. By contrast, Figure EC.1b shows a P_{16} line network for which the baseline routing becomes infeasible. The baseline routing satisfies the nominal physical capacity constraints, but handling causes line 8 to spend 1333 of its 1440 available time units handling parcels, reducing the effective capacity of arc $(1,6)$ to 146.3, below the 536 units routed on that arc. Lastly, for comparison, a line with one vehicle, $T = 60$, and a total handling workload of 80 time units is temporally infeasible, regardless of vehicle capacity.

The strengthened SDP relaxation

As outlined in Section 5, for an endpoint γ_b, we begin with the following SDP relaxation of the localized endpoint problem:

$$\min \quad \sum_{l\in\mathcal{L}} C_l\langle M_l, Z_l\rangle \tag{EC.2a}$$

$$\text{s.t.} \quad x \in \mathcal{X}_b^{F_c}, \quad z_l = E_l x, \quad y_l = Ta_l - e_l^\top z_l, \qquad l \in \mathcal{L}, \tag{EC.2b}$$

$$Ta_l s_l - e_l^\top w_l = 1, \quad Ta_l w_l - Z_l e_l = z_l, \qquad l \in \mathcal{L}, \tag{EC.2c}$$

$$\begin{pmatrix} Z_l & w_l \\ w_l^\top & s_l \end{pmatrix} \succeq 0, \qquad l \in \mathcal{L}. \tag{EC.2d}$$

The flow vector x describes the routing, while z_l, y_l, s_l, w_l and the symmetric matrix Z_l are auxiliary variables associated with each line. Here, $z_l = (\boldsymbol{h}_l, \boldsymbol{X}_l) = E_l x$ collects the handling workloads and incoming onboard flows at the hubs of line l, and e_l selects the handling coordinates so that $e_l^\top z_l$ is their sum. As in Section 5, we can express the bilinear numerator $\boldsymbol{h}_l^\top \boldsymbol{X}_l$ in terms of z_l using the following matrix M_l:

$$M_l = \frac{1}{2}\begin{pmatrix} 0 & I \\ I & 0 \end{pmatrix}, \qquad z_l^\top M_l z_l = \boldsymbol{h}_l^\top \boldsymbol{X}_l,$$

where I is the identity matrix of dimension $|\mathcal{N}(l)|$. At an exact lift, $s_l = 1/y_l$, $w_l = z_l/y_l$, and $Z_l = z_l z_l^\top / y_l$, so the lifted objective equals $r(x)$. The base SDP retains the positive semidefinite constraint and the linear identities implied by these relations, but drops the rank-one requirement. Consequently, the lifted variables need not satisfy these product identities, allowing the objective to underestimate the residual cost.

To limit deviations from these identities, we use McCormick envelopes. For instance, consider $w_{lj} = z_{lj}/y_l$, or equivalently $z_{lj} = y_l w_{lj}$. While this identity need not hold in the relaxed SDP, we can add the following constraints, where an underline and overline denote a variable's lower and upper bounds, respectively:

$$\begin{aligned} z_{lj} &\geq \underline{y}_l w_{lj} + \underline{w}_{lj} y_l - \underline{y}_l \underline{w}_{lj}, \\ z_{lj} &\geq \overline{y}_l w_{lj} + \overline{w}_{lj} y_l - \overline{y}_l \overline{w}_{lj}, \\ z_{lj} &\leq \overline{y}_l w_{lj} + \underline{w}_{lj} y_l - \overline{y}_l \underline{w}_{lj}, \\ z_{lj} &\leq \underline{y}_l w_{lj} + \overline{w}_{lj} y_l - \underline{y}_l \overline{w}_{lj}. \end{aligned} \tag{EC.3}$$

We impose these inequalities for all $l \in \mathcal{L}$ and every coordinate j of z_l. We similarly impose McCormick envelopes for $Z_{ljk} = z_{lj} w_{lk}$ for every ordered pair (j, k). Since Z_l is symmetric, this also imposes the envelopes for $Z_{ljk} = z_{lk} w_{lj}$. Naturally, these McCormick inequalities become stronger as the variable bounds tighten. We therefore perform optimization-based bound tightening (OBBT) on y_l and the coordinates of z_l by minimizing and maximizing them over convex relaxations that include the endpoint budget and incumbent cutoff. A strong incumbent helps restrict the region over which these bounds are computed. We impose the resulting bounds and retain the bounds on boarding and unloading aggregates from preliminary tightening. Since z_l is nonnegative and the denominator bounds are strictly positive, we also obtain bounds on the fractional variables:

$$\begin{aligned} &0 < \underline{y}_l \leq y_l \leq \overline{y}_l, \qquad \underline{z}_{lj} \leq z_{lj} \leq \overline{z}_{lj}, \\ &\frac{1}{\overline{y}_l} \leq s_l \leq \frac{1}{\underline{y}_l}, \qquad \underline{w}_{lj} := \frac{\underline{z}_{lj}}{\overline{y}_l} \leq w_{lj} \leq \frac{\overline{z}_{lj}}{\underline{y}_l} =: \overline{w}_{lj}. \end{aligned} \tag{EC.4}$$

In addition, Section 4 gives a lower bound for $r_l(x)$ based on the unloading flow $U_i^l = \sum_k u_i^{kl}$. We retain the restriction $U_j^l \leq X_{ij}^l$ on each incoming line arc (i, j), which preserves an optimum as discussed in Section 4, and add

$$\langle M_l, Z_l \rangle \geq 0, \qquad \langle M_l, Z_l \rangle \geq \frac{\beta}{y_l} \sum_{i \in \mathcal{N}(l)} (U_i^l)^2, \qquad l \in \mathcal{L}. \tag{EC.5}$$

This ensures that the lifted residual is bounded below by the convex underestimator used in the SOCP relaxation. After adding the cuts described in Section 5, we get the following SDP that we solve in practice.

$$
\begin{aligned}
\ell_b = \min_{x,z,y,s,w,Z} \quad & \sum_{l\in\mathcal{L}} C_l\langle M_l, Z_l\rangle \\
\text{s.t.} \quad & \text{base constraints (EC.2b)–(EC.2d),} \\
& \text{variable bounds described above, including (EC.4),} \\
& \text{envelopes (EC.3) and the analogous envelopes for } Z_{ljk}, \\
& U^l_j \le X^l_{ij} \quad ((i,j)\in\mathcal{A}(l),\ l\in\mathcal{L}), \\
& \text{residual inequalities (EC.5),} \\
& \ell^{(b)}_{lq} \le q^\top z_l \le u^{(b)}_{lq}, \\
& \min\left\{\frac{\ell^{(b)}_{lq}}{\underline{y}_l}, \frac{\ell^{(b)}_{lq}}{\overline{y}_l}\right\} \le q^\top w_l \le \max\left\{\frac{u^{(b)}_{lq}}{\underline{y}_l}, \frac{u^{(b)}_{lq}}{\overline{y}_l}\right\}, \\
& \text{McCormick envelopes for } q^\top z_l = y_l(q^\top w_l), \\
& q^\top Z_l q \le (\ell^{(b)}_{lq} + u^{(b)}_{lq}) q^\top w_l - \ell^{(b)}_{lq} u^{(b)}_{lq} s_l, \\
& f_{\text{lin}}(x) + \frac{T}{2(\alpha+\beta)} \sum_l C_l(T a_l s_l - 1) \le g_c + \gamma_b, \\
& f_{\text{lin}}(x) + \frac{T}{2(\alpha+\beta)} \sum_l C_l(T a_l s_l - 1) + \sum_l C_l\langle M_l, Z_l\rangle \le F_c.
\end{aligned}
\tag{EC.6}
$$

The constraints apply to every relevant line, coordinate, and selected direction. At an exact lift, the last two inequalities are the endpoint budget $g(x) \le g_c + \gamma_b$ and incumbent cutoff $F(x) \le F_c$.

For all experiments, we begin with $B = 12$ intervals and focus refinement on the weakest stair, its neighbors, and other intervals close to the minimum. In each adaptive round, we either split the selected intervals into four or strengthen their endpoint SDPs by generating up to three additional directions for each of up to three selected lines. We apply OBBT to the new projections before adding their corresponding envelopes and cuts. The procedure stops after at most six adaptive rounds, or earlier if a strengthening pass produces negligible improvement in the bound. We solve the SDPs using MOSEK and the OBBT subproblems using Gurobi, with parallel OBBT where applicable.

Appendix C: Additional Instances Information

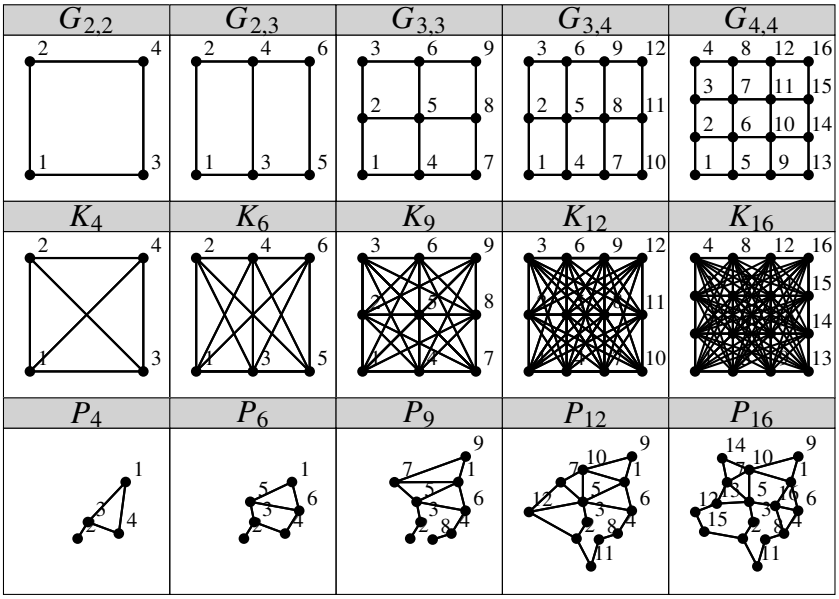
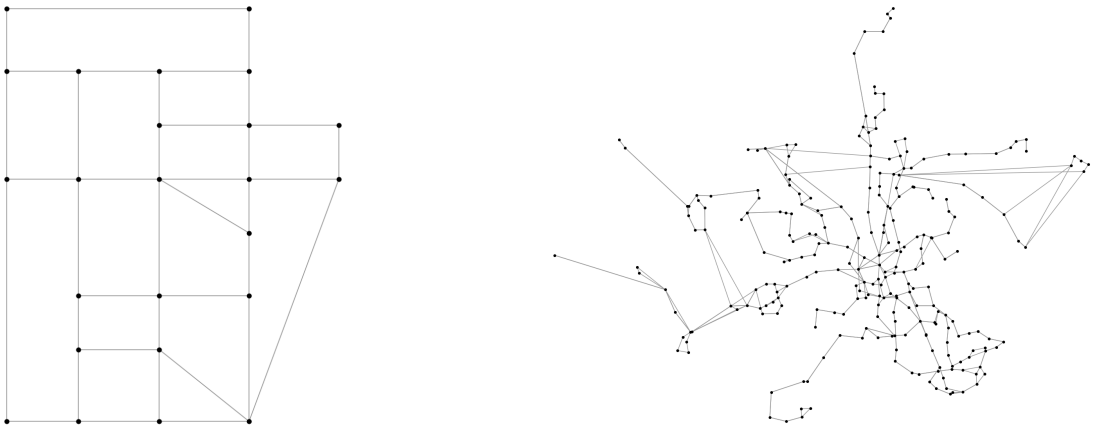


Figure EC.2 **PTNs of the 15 synthetic instances.**



(a) Sioux Falls (SF) (b) Göttingen (GöVB)

Figure EC.3 **Real-world PTN instances used in the experiments.**